Complex Taxis-Behavior in a Novel Bio-Inspired Robot Controller

Thomas Schmickl, Heiko Hamann, Jürgen Stradner, Ralf Mayet, and Karl Crailsheim
Artificial Life Lab of the Department of Zoology, Karl-Franzens University Graz, Universitätsplatz 2, A-8010 Graz, Austria
thomas.schmickl@uni-graz.at

Abstract

In swarm robotics, robots with only poor computational equipment are often used. Additionally, the precision of their actuators and sensors is rather poor. This causes a challenge in the construction of controllers able to achieve complex behaviors on such robotic systems. Here we describe a novel bio-inspired concept of a robot control paradigm, which is inspired by the information-processing of simple microorganisms. The basic idea is that we use a roughly abstracted model of inter-cellular signal emission and signal processing to control the movement behavior of a two-wheeled autonomous robot. Many unicellular organisms are able to perform taxis-behavior (phototaxis, chemotaxis, etc.) without having sophisticated sensor equipment and without possessing neuronal structures. Our Artificial Homeostatic Hormone System (AHHS) mimics primitive chemical signal networks and is able to achieve taxis-behavior with little computational cost. In this article the controller is analyzed in a simple mathematical model and additional tests are performed on a more sophisticated multi-agent simulation of robotic hardware and the controller is implemented on real robotic hardware.

INTRODUCTION

In swarm robotics (Beni, 2005; Şahin, 2005) simple and inexpensive robotic hardware is used frequently. Such robotic systems often have limited computational abilities and their sensors and actuators are rather imprecise. Also memory is often limited and therefore the minimal hardware equipment cannot easily be compensated by extensive software concepts such as data filtering, managing a world-model or by simultaneous localization and mapping (SLAM) of the environment. Thus, it is a challenging task to generate controllers that allow the generation of adaptable complex behaviors. In addition, evolutionary robotics (Floreano et al., 2008) is a concept to automatically design 'simple' robot controllers with algorithms of evolutionary computation, to explore the behavior space of the robots and to generate the desired behaviors.

Many microorganisms, that have only limited sensor precision and do not have neuronal systems to process information, show an impressive ability to perform complex and/or target-oriented behaviors (taxis). For example, a unicellular algae (Bound and Tollin, 1967) performs phototaxis with just one photo-sensitive eye-spot and just a single actuator (flagellum). Similar capabilities are found in many bacteria (Khan et al., 1995; Darnton et al., 2007). Also, multi-cellular aggregation (colonies) of simple cells are able to coordinate their joint motion to collectively approach the source of a stimulus (e.g., phototaxis in *Volvox*, Holmes (1903)).

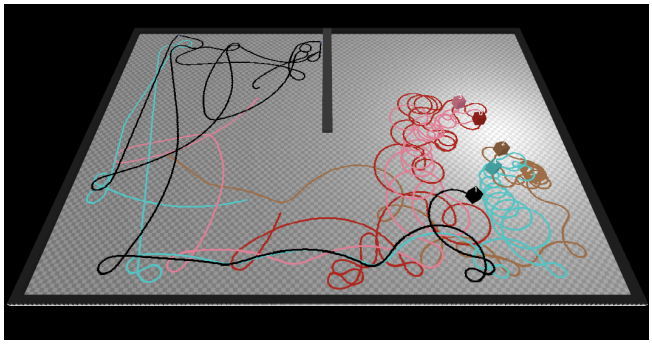

Figure 1: Five robots showing phototactic behavior with AHHS controller.

The internal processes of cells can be interpreted as computational processes as reported by Bray (2009). This 'non-cognitive' method (i.e., single cells have no neurons, hence, it is an anti-connectionist approach) of information processing was applied many decades ago by Grey Walter (Grey Walter, 1950, 1951) to control a simple robot. The behaviors reported in these papers are similar to this work, only we are modeling internal cell processes explicitly. In previous studies (Schmickl and Crailsheim, 2009; Hamann et al., 2010b,a), we suggested a simple difference-equation based model of the internal signal processing of uni-cellular organisms, which we call Artificial Homeostatic Hormone System (AHHS). In such systems, representing rough abstractions of biological physiological models, the difference-equation model controls the way of how a robot acts based on sensory input.

In the model we assume that the inner body of the robot is compartmentalized. Specific compartments are associated with certain components of the robot's real body. In

each compartment, the model tracks the dynamics of virtual chemical substances, which represent chemical cell signals in real organisms. These chemical substances can diffuse to neighboring compartments and they decay proportionally to their current concentration over time. Some of them are produced at constant rates as well, leading to homeostatic set points (equilibria) that are approached after an initial transient. Some of these signals affect actuators (e.g., wheels), leading to unstimulated behavioral modes of the organism. Sensor excitation by environmental stimuli result in local disturbances in the hormone equilibria, for example, by sudden secretion of one of the chemical signals (hormones). As hormone levels affect actuators, changing hormone concentrations may change the robot's behavior. This stimulated behavior lasts until the 'abnormal' sensor excitation has ceased and the hormone levels have approached the previous homeostatic settings again. A set of hormone-to-hormone interactions can enhance the behavioral repertoire of the robot by providing more complex forms of sensor-to-actuator linkage via the virtual hormone reaction networks.

To demonstrate the abilities of AHHS controllers in producing interesting behavioral patterns even with limited computational and with limited sensor equipment, we aimed to mimic taxis behavior that is found in very primitive lifeforms (e.g., some bacteria).

The bacterium *Esherichia coli* shows interesting behavior in finding attractive habitats by chemotaxis. The bacterium is propelled by several flagella (actuators), which have two modes of turning: clockwise (CW) and counter-clockwise (CCW). The CCW motion allows the organism to swim almost in straight trajectories and the CW motion of some flagella disturb the synchrony among the bundle of all flagella. This leads to a so called 'tumbling mode' of movement, where the organism almost randomly changes its direction (Khan et al., 1995; Darnton et al., 2007). Chemoreceptors that react to attractants in the environment suppress those cell-internal chemical signals which finally alter the rotation of flagella to the CW mode. In absence of these attractants, the CW mode is not suppressed that much, which leads to a higher probability and longer duration of the 'tumbling mode'.

This way, the organism is able to ascend in an attractive chemical gradient in a way that was found to be a very robust control mechanism (Alon et al., 1999; Yi et al., 2000). This approach of taxis is rather different from those approaches frequently used in mobile robotics, for example the famous Braitenberg vehicles (Braitenberg, 1984). For example, using just one single sensor is comparable to 'vehicle 1'. But the functionality of the taxis-behavior is not existent in 'vehicle 1', which rather speeds up or slows down depending on the current sensor intensity. When searching for the functionality of taxis, which is provided in our approach, a comparison with 'Braitenberg vehicles 2 and 3 (fear, aggression and love)' makes more sense. But here, the inner structure of the controller does not correspond. In contrast to these Braitenberg vehicles, our AHHS controller uses just one sensor, thus no gradient-ascent based on differences between parallel sensor values is used. Furthermore, there is no explicit implementation of any kind of 'seeking-behavior': Neither does the robot rotate with a directional sensor measuring light intensity until it finds a maximum in a particular direction that it then approaches directly, nor does it use any explicit memory storage of past sensor values or an explicit 'world model'. In contrast, we claim that in our solution, the robot, its position in the world (relative to the light optimum) and the trajectory itself serve as some kind of memory and as some kind of world model. This approach is rather unique.

In the study presented here, we investigate how an AHHS controller can be programmed to perform a comparably simple behavior with similar simple mechanisms. As most cheap robots are lacking real gas detectors (chemo-sensors) we wanted our focal robot to pursue a different but comparable task, that is phototaxis:

Our focal robot is equipped with two wheels and just one sensor on the right hand side of the robot. In this first controller example, this sensor is discrete and either passes a 1 (light perceived) or a 0 (no light perceived) to the controller. This 'binary' controller is able to detect whether it points towards the light or not, thus offering some directionality. In a second controller, we assumed that the sensor cannot determine this directionality, instead it can just report the local illuminance at the robot's current position. In contrast to the first controller, here the sensor reports a graduated output value proportionally to the current local illuminance. The task for the robot is to drive towards a light (phototaxis).

For a fixed topology with two wheels and a sensor on the right side of the robot, there are four potentially reasonable ways of programming a reactive agent: Without any sensory input the robot moves in right turns and sensory input either reduces the radius of the turns or it increases the radius. The other option is to let the robot move in left turns without sensory input and sensory input either reduces the radius of the turns or it increases the radius. The methods with standard right turns are gradient descends and the left turns lead to gradient ascends. The method of decreasing the turn radii leads to trajectories with many loops. We call this method *positive steering* because the robot steers by intensifying the standard turn direction. The method of increasing the turn radii or even changing the turn direction leads to waved or straight trajectories. We call this method *negative steering* because the robot steers by decreasing or inverting the standard turn.

AHHS controllers

In both of the reported controllers, we assumed that a basic 'forward-driving' hormone H^f is produced (in the following: forward hormone) in both compartments of the robot

at rate α. This hormone activates the motors. The main difference between these two controllers is the asymmetric production rate (α_l in the left compartment, $alpha_r$ in the right compartment, with $\alpha_l \neq \alpha_r$) in case of the first controller. The second controller has a symmetric production rate ($\alpha_l = \alpha_r = \alpha$). Thus, the levels of the forward hormone are equal in the 'normal' state, the robot basically drives in straight lines. Such an AHHS controller can easily be combined with a collision-avoidance system, as it was discussed in (Schmickl and Crailsheim, 2009; Stradner et al., 2009).

First AHHS controller

In our first AHHS controller, we assumed that the robot is equipped with a sensor that is able to determine whether it points towards the light source (within an angular threshold of $\pm 90^o$ around the sensor center). If this is the case, the sensor triggers the production of a light-dependent hormone H^l (in the following: light hormone). The light hormone interacts with the forward hormone H^f by blocking (decreasing) it. Thus, the hormone level in the compartment, that corresponds to the side of the light-sensor, is decreased by the light hormone and the robot starts to turn in curves towards this side. This first approach was inspired by the phototactic behavior of *Euglena gracilis* (Bound and Tollin, 1967), which rotates around its axis until a shading pigment shades the organism's eyespot. This is only the case, if the organism is oriented correctly towards the stimulus (light) source. In this case, all phobic responses disappear and the organism moves towards its target. In our case, also just one binary and directional sensor is available and the 'body' of the robot acts as a shading device.

We chose a system of difference equations to model the agent. It is assumed that the agent moves in a plane. The agent's position is given by $\mathbf{x}$ and updated by

$$\frac{\Delta \mathbf{x}}{\Delta t} = \begin{pmatrix} \cos\phi(t) \\ \sin\phi(t) \end{pmatrix} v, \tag{1}$$

for the agent's heading ϕ and a constant velocity $v > 0$. The change of the heading is defined by

$$\frac{\Delta \phi}{\Delta t} = \left((H_l^F(t) - H_l^L(t)) - (H_r^F(t) - H_r^L(t)) \right) \theta, \tag{2}$$

for the value of the forward hormone in the left compartment H_l^F (right compartment H_r^F), the value of the light hormone in the left compartment H_l^L (right compartment H_r^L), and a parameter θ called steering intensity that defines the intensity of the turns related to the difference in hormones in the tow compartments. The dynamics of the forward hormone H^F are given by

parameter	value
hormone production left α_l	0.11 [1/time unit]
hormone production right α_r	0.1 [1/time unit]
hormone decay β	0.04 [1/time unit]
hormone diffusion D	0.001
agent velocity v	0.01 [space unit/time unit]
sensor scale factor σ	0.03
steering intensity θ	0.1
sensor offset δ	45^o

Table 1: Standard parameters for the model of the first controller.

$$\frac{\Delta H_l^F}{\Delta t} = \alpha_l - \beta H_l^F(t) + D(H_r^F(t) - H_l^F(t)), \tag{3}$$

$$\frac{\Delta H_r^F}{\Delta t} = \alpha_r - \beta H_r^F(t) + D(H_l^F(t) - H_r^F(t)), \tag{4}$$

for hormone production rates α_l (left compartment) and α_r (right compartment), decay rate β, and diffusion constant D. The update rule of the light hormone H^L is

$$\frac{\Delta H_l^L}{\Delta t} = -\beta H_l^L(t) + D(H_r^L(t) - H_l^L(t)), \tag{5}$$

$$\frac{\Delta H_r^L}{\Delta t} = -\beta H_r^L(t) + \sigma S(t) + D(H_l^L(t) - H_r^L(t)), \tag{6}$$

for a sensor input $S(t)$ and the sensor scale factor σ.

The sensor returns a 1, if it points towards the light source (within an angular threshold of $\pm 90^o$ around the sensor center). Otherwise it returns a 0. This is defined by the scalar product:

$$S(t) = \begin{cases} 1 & \text{if } \left| \arccos\left(\|\mathbf{x}(t)\| \cdot \begin{pmatrix} \cos(\phi(t)+\delta) \\ \sin(\phi(t)+\delta) \end{pmatrix} \right) \right| > 90^o \\ 0 & \text{else.} \end{cases} \tag{7}$$

The standard parameters, that were used, if not stated explicitly, are given in Table . With this model we generated examples of trajectories by solving it numerically. Examples of three trajectories are shown in Fig. 2. These trajectories clearly show the two different strategies of positive and negative steering by changing the steering intensity parameter θ (a convoluted trajectory compared to waved and straight trajectories).

The model was also used to do extensive scans of parameter intervals. For example, an interesting behavior was found for the sensor scale factor σ that indicates complex behavior.

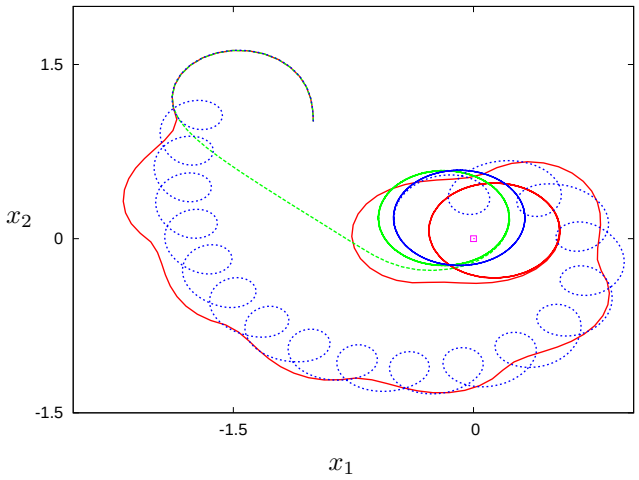

Figure 2: Examples of three trajectories with different parameter settings. The agent starts at $\mathbf{x} = (-1, 1)$ with heading $\phi = 90^o$ (north). The maximum of the light gradient is located at $(0, 0)$. The blue trajectory is an example of positive steering ($\theta = 0.1$). The green ($\sigma = 0.25$) and red ($\sigma = 0.01$) trajectories are examples of negative steering ($\theta = -0.1$).

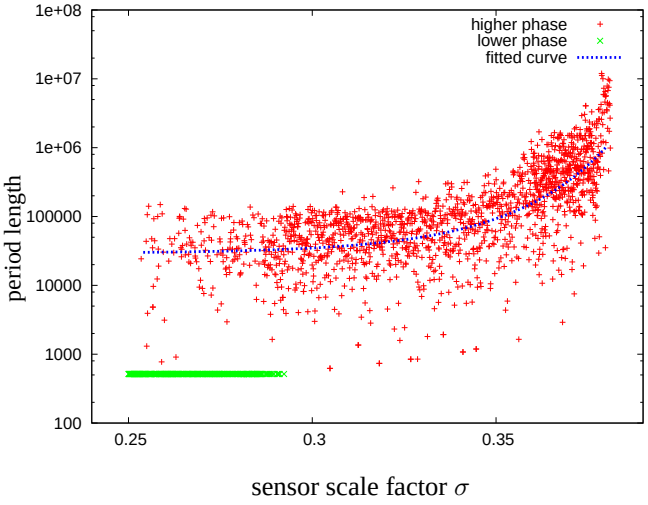

Figure 3: Scan over the sensor scale factor σ showing its influence on the length of the asymptotic period length. The green points correspond to the smallest possible period, red points correspond to rather complex periodic behaviors. The fitted blue curve is double exponential.

The sensor scale factor influences the radius of the circular behavior to which the robot converges to (i.e., the period length). Results are shown in Fig. 3 that indicate a complex relation (double exponential increase) between the sensor scale factor and the period length.

Second AHHS controller

In this example, we assumed a photo-receptor which is mounted on top of the robot, so that it has no directionality at all. It just can report the local luminance in a graduated manner: The higher the local luminance, the higher is the reported sensor value. This sensor value produces a light-dependent hormone in one of the two compartments of the AHHS controller, which breaks down the forward-driving hormone. As the sensor produces this hormone proportionally to the local illuminance, the forward-driving hormone level is lowered also in a proportional level, leading to smaller curve radii in higher illuminated areas. This rotation-behavior, changing the orientation of the robot frequently and decreasing the net movement speed of the robot, is inspired by the mechanisms of chemotaxis reported with *Escherichia coli*.

The agent's position update of this second controller is defined as in Eq. 1. The dynamics of heading ϕ is now given just by the difference of the forward hormone:

$$\frac{\Delta\phi}{\Delta t} = (H_l^F(t) - H_r^F(t))\theta. \tag{8}$$

The update rule of the forward hormone is similar to the definition above, except that now it is reduced by the light hormone H^l:

$$\frac{\Delta H_l^F}{\Delta t} = \alpha - \beta H_l^F(t) + D(H_r^F(t) - H_l^F(t)) - \gamma H_l^L(t), \tag{9}$$

$$\frac{\Delta H_r^F}{\Delta t} = \alpha - \beta H_r^F(t) + D(H_l^F(t) - H_r^F(t)) - \gamma H_r^L(t), \tag{10}$$

for production rate α (now symmetrically defined), diffusion constant D, decay rate β, and hormone-induced decay γ.

The update of the light hormone is defined as given by Eq. 6. The sensor input is now a continuous value which is a direct measurement of the local light intensity. The light gradient is simply defined by the reciprocal of the distance of the agent to the origin which is here the position of the light source:

$$S(t) = 1/\|\mathbf{x}(t)\|, \tag{11}$$

for agent position $\mathbf{x}$. The standard parameters, that were used, if not stated explicitly, are given in Table . An example of an agent's trajectory for this second controller is shown in Fig. 4.

We used this model to do extensive parameter interval scans. Such scans are the specialty of such abstract mathematical models due to the small computational cost of solving them. We just need a valid metric to (automatically) measure the performance of the parameter set. One possible

parameter	value
hormone production left α	0.1 [1/time unit]
hormone decay β	0.04 [1/time unit]
hormone diffusion D	0.03
agent velocity v	0.01 [space unit/time unit]
sensor scale factor σ	0.2
steering intensity θ	0.3
hormone-induced decay γ	0.003 [1/time unit]

Table 2: Standard parameters for the model of the second controller.

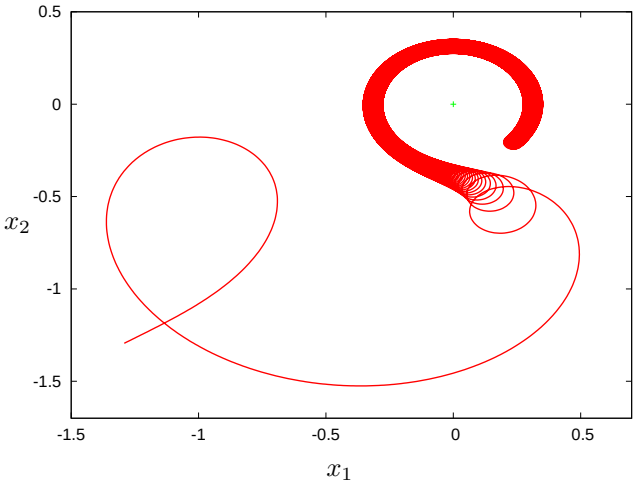

Figure 4: An example of an agent's trajectory for the second controller.

measure of the quality of the gradient ascent is the distance to the maximum during the asymptotic and periodic behavior of the agent. In Fig. 5 we present scans over the diffusion constant D, the steering intensity θ, and the hormone-induced decay rate γ for three different initializations of the agent position. For each parameter value six distances of the trajectory to the maximum of the light gradient during the last 3000 time steps are plotted (3000, 2500, ..., 500, 0 time steps before the numerical integration was stopped). Clearly two phases are detected. The distances above a distance of 100 correspond to the maximal possible distance that can be obtained by a robot (by driving in a straight line). Close to optimal parameter settings are found by choosing parameters with low distances. However, the parameters are not fully mutually independent.

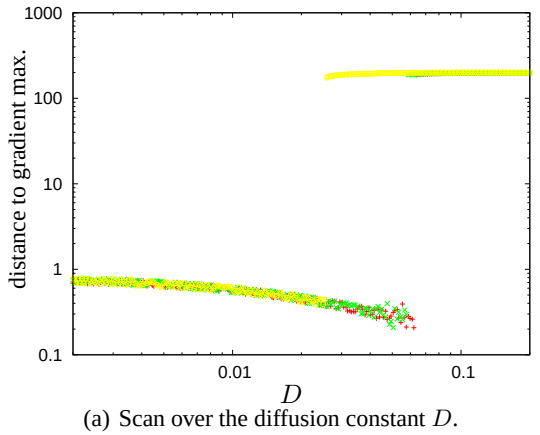

(a) Scan over the diffusion constant D.

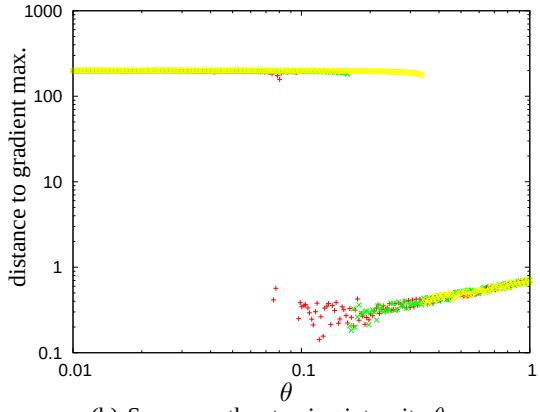

(b) Scan over the steering intensity θ.

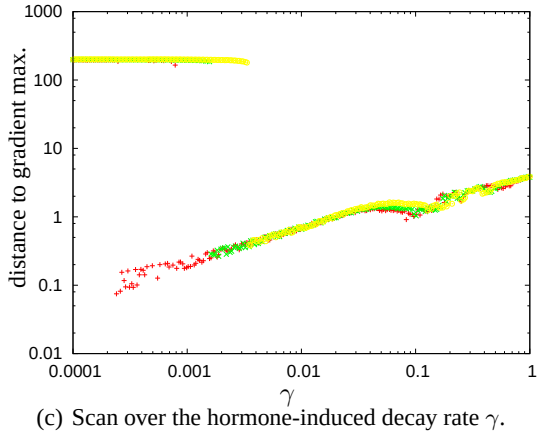

(c) Scan over the hormone-induced decay rate γ.

Figure 5: Scan over different parameters showing the distance to the maximum of the gradient of 6 time steps during the asymptotic behavior (3000, 2500, ..., 500, 0 steps before stopping to iterate) for three different initializations of the agent's positions (indicated by different colors). The distances above 100 correspond to the maximal possible distance that is obtained by driving in a straight line. Clearly two phases are detected.

Multi-agent implementation of the second AHHS controller

We tested the second AHHS controller in a multi-agent simulation of real robotic hardware, because we think that this controller is especially interesting for robotics: It allows a gradient ascent without any explicit memory of past sensor values and without any directionality of the used sensor. To test whether this concept works also in a more realistic environment (walls, obstacles, collision avoidance of robots) compared to the mathematical model described above, we implemented the AHHS controller in an individual based multi-agent simulation as well. In our multi-agent simulation, each robot can detect nearby obstacles through 2 IR sensors which are mounted laterally. These distance sensors emit a 'collision stress' hormone, which additionally activates the motor on the ipsi-lateral side. This leads to a turning away from the obstacle. This collision-avoidance behavior was implemented in an AHHS controller in (Schmickl and Crailsheim, 2009) where it is described in more detail. The focal questions for our experiment described here are: Will the collision-avoidance interfere with the phototactic behavior of our above-mentioned second AHHS controller? Will the phototactic behavior be adaptive to environmental fluctuations? Will sensor noise affect the system? To investigate these questions we tested the combined AHHS controller (collision avoidance and phototaxis) in a simulated robotic arena which was bound by an arena wall. All sensor data was affected by $\pm 25\%$ uniform random noise. To test the adaptability of the robots, we switched the position of the simulated light source to the other side of the arena, as soon as the robot approached the first optimum.

As can be seen in Fig. 6(a), the robot performs 'normal' collision avoidance behavior successfully when no light spot is present in the arena. As soon as the light spot is forming a gradient pointing towards the lower left corner of the arena, the robot starts to approach it with its characteristic phototactic behavior, see Fig. 6(b). After the robot approached the light spot, we switched the lightspot's position at a sudden and the robot changed its behavior and started to approach the new optimum, see Fig. 6(c). Fig. 7 shows the dynamics of the forward-driving hormone and of the light-induced hormone in the last two phases of the experiment. It is clearly visible how the robot maximizes the light hormone, thus it approaches the light spot, which, in turn, leads to a lowering of the forward-driving hormone.

To perform a further test of this controller in the multi-agent simulator, we performed additionally a test run, which is shown in Fig. 1. In this run, the light spot was placed at the right side of a lengthy arena and 5 robots started simultaneously at the left side of the arena. A wall narrows down the possible paths from the left to right side of the arena and the robots had to avoid each other, as well as the surrounding outside wall. As the trajectories in Fig. 1 demonstrate the robots successfully managed to approach the light spot. The robot-to-robot interactions led to even more complex trajectories compared to those of the single-robot runs. We assume that such swarm effects can be exploited to kick robots out of circular trajectories that surround local optima. This will be tested in future studies.

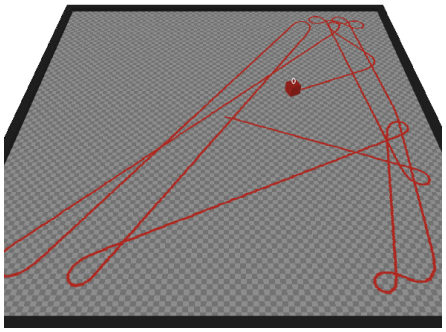

(a) No light spot in the habitat.

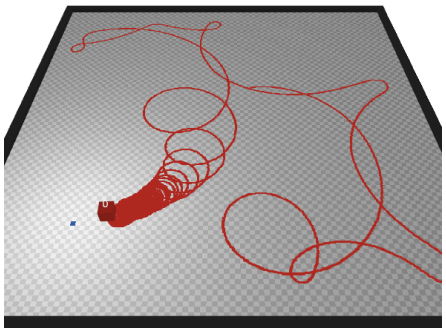

(b) Light spot in the lower left corner.

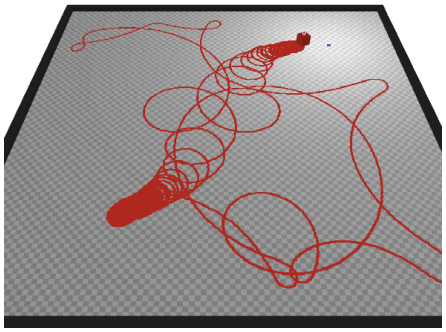

(c) Light spot moved to the upper right spot.

Figure 6: Trajectories of robots in three phases of our 'disturbance' experiment. Without any light spot, the robot performs only collision avoidance. As soon as the light spot is in the left lower corner, the robot approaches it in the characteristic phototactic behavior. As soon as the light spot is shifted to the right upper arena corner, the robot changes its behavior and approaches the new optimum.

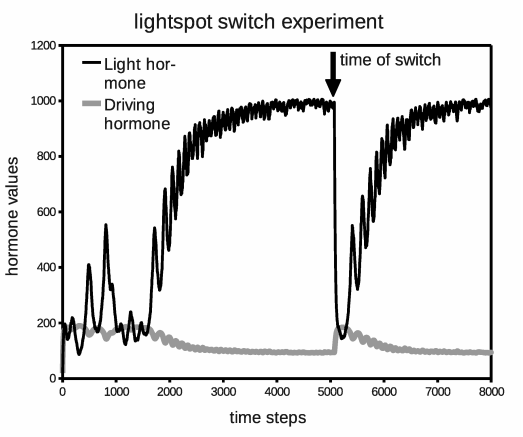

Figure 7: Hormone values in the AHHS controller that governed the robot's behavior in the 'disturbance' experiment, which is depicted in figure 6.

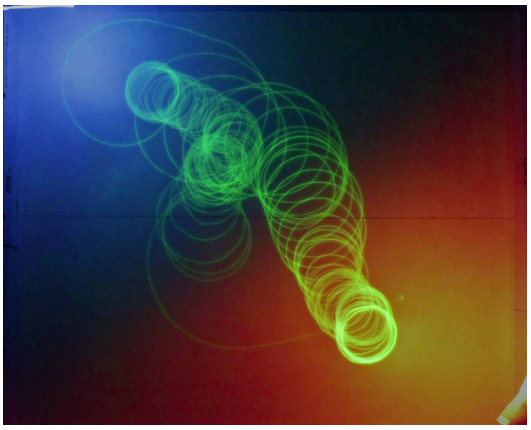

Figure 8: Composite image of the robotic implementation of the light-seeking AHHS in an e-puck robot. The two light emitters can be seen in the top left and bottom right corners. The robot trail, here captured using a phosphorescent paint, shows the spiral-way approach to the top left corner and the bottom right corner.

Implementation of the AHHS in robotic hardware

Based on the results we obtained from our simulation studies, we implemented the algorithm of the second AHHS controller (described above) on a robotic platform. We used an 'e-puck' robot (Mondada et al., 2009) for this experiment. The robot was equipped with only one light-sensor on top, pointing upwards. Therefore, the light sensor reports local luminance without any directional information. Also, the robot is equipped with two wheels (differential drive). The 'forward hormone' is steadily produced and decays proportionally, establishing an equilibrium that in turn determines the robots general forward speed. The 'light hormone' of the AHHS is emitted in response to light sensation, increasing the decay rate of the 'forward hormone' to slow the right wheel, thus inducing a curved trajectory. For the AHHS, we used the following parameterization: $\beta_1 = 0.04$, $\beta_2 = 0.04$, $D = 0.015$, $\alpha = 0.1$, $\gamma = 0.03$, and $\sigma = 0,055$. The light sensor reports sensor values between 0 (absolute darkness) and 1 (maximum luminance) with a noise factor of about 0.2. Because the arena was bounded by a wall, we implemented a collision-avoidance behavior based on the 8 IR proximity sensors of the e-puck robot. This behavior overruled the AHHS control when the robot approached a wall. In (Stradner et al., 2009), we showed that this kind of collision-avoidance behavior can also be built using an AHHS control.

For this experiment, we used an arena ($2.0\text{m} \times 1.8\text{m}$) with two light emitters in opposing corners (top left and bottom right). At first, only one emitter (top left) was switched on. The robot was placed directly under the other, switched off, light source with a heading pointing away from the light optimum. The robots objective was to navigate to the brightest spot in the arena, directly under the light emitter (top left). After the robot had reached the light spot, the light emitter was switched off, while the other emitter was switched on (bottom right). The robots task was now to locate and navigate to the new light optimum.

Figure 8 shows, that the robot (running the AHHS) performs the spiral-way target approach towards the light gradient successfully. It can be seen that the light sensor's noise is significantly reduced in both hormone levels, thus enabling the smooth spiraling movement of the robot.

CONCLUSIONS AND FUTURE WORKS

Conclusions

We have successfully demonstrated that a simple bio-inspired AHHS controller can be used to achieve phototactic behavior in autonomous robots. The controller is simple, so that it can be easily analyzed and studied with mathematical differential-equation models. Using this technique we analyzed the emerging phototactic behavior of two different controller setups, both based on different AHHS configurations. Both setups managed to perform phototaxis with just one single illuminance sensor, having a different sensor characteristic in each setup. Our mathematical analysis shows that the more interesting (and more complex) behavioral patterns can be produced with the second controller. This is especially interesting, because in this controller setup, the sensor offers no directionality and past information is never explicitly stored in a memory system. This means that the robot does not simply compare old and new sensor data and performs no memory-based gradient ascent. The behavior also differs significantly from classical Braitenberg vehicle approaches (Braitenberg, 1984).

One important aspect of simple mathematical models is that they allow exhaustive parameter sweeps in reasonable computational time. From our performed parameter sweeps

we conclude that the modeled AHHS controllers have a defined, but wide, range of parameters that lead to the desired phototactic behavior. The tests in the multi-agent simulation show, that this phototactic behavior can be performed, even with an underlying obstacle avoidance, with a more realistic robotic habitat and with a huge amount of sensor noise. And even multiple and frequent robot-to-robot interactions did not significantly impair the robot's ability to approach the desired target. In addition, the 'disturbance experiments' showed that the emerging phototactic behavior is stable on the one hand and flexible on the other hand. The AHHS controller has also been shown to work on real robotic hardware, in our case the e-puck robot. It performed a smooth spiral-way target approach similar to those in the multi-agent simulation. Furthermore it could adapt to the changing environment, when the light source switched places.

Future Works

In the future, we plan to use Evolutionary Computation to optimize parameter sets of our AHHS systems. We plan to implement a novel way of Artificial Evolution, so that evolutionary operators can 'create' new hormones and new sensor-to-hormones and hormones-to-actuator links. In addition, we plan to extend the system to multi-modular robotics, so the virtual hormones can be exchanged by linked robotic modules. This way, we plan to mimic the evolutionary step from uni-cellular to multi-cellular organism, like it happened several times in the natural evolution of life forms.

ACKNOWLEDGMENTS

We were supported by the following grants: EU-IST FET project 'I-SWARM', no. 507006 and the FWF research grant no. P19478-B16, EU-IST FET project 'SYMBRION', no. 216342, EU-ICT project 'REPLICATOR', no. 216240.

References

Alon, U., Surette, M. G., Barkai, N., and Leibler, S. (1999). Robustness in bacterial chemotaxis. *Nature*, 397:168–171.

Beni, G. (2005). From swarm intelligence to swarm robotics. In Şahin, E. and Spears, W. M., editors, *Swarm Robotics - SAB 2004 International Workshop*, LNCS, pages 1–9, Santa Monica, CA.

Bound, K. and Tollin, G. (1967). Phototactic response of *euglena gracilis* to polarized light. *Nature*, 216:1042–1044.

Braitenberg, V. (1984). *Vehicles: experiments in synthetic psychology*. MIT Press, Cambridge, MA.

Bray, D. (2009). *Wetware: A Computer in Every Living Cell*. Yale University Press.

Şahin, E. (2005). Swarm robotics: From sources of inspiration to domains of application. In Şahin, E. and Spears, W. M., editors, *Swarm Robotics - SAB 2004 International Workshop*, volume 3342 of *LNCS*, pages 10–20, Berlin, Germany. Springer-Verlag.

Darnton, N. C., Turner, L., Rojevsky, S., and Berg, H. C. (2007). On torque and tumbling in swimming *escherichia coli*. *Proceedings of the National Academy of Sciences*, 189:17561764.

Floreano, D., Husbands, P., and Nolfi, S. (2008). Evolutionary Robotics. In Siciliano, B. and Oussama, K., editors, *Handbook of Robotics*, chapter 61, pages 1423–1452. Springer, Berlin.

Grey Walter, W. (1950). An imitation of life. *Scientific American*, 182(5):42–45.

Grey Walter, W. (1951). A machine that learns. *Scientific American*, 185(2):60–63.

Hamann, H., Stradner, J., Schmickl, T., and Crailsheim, K. (2010a). Artificial hormone reaction networks: Towards higher evolvability in evolutionary multi-modular robotics. In *Alife XII*. MIT Press.

Hamann, H., Stradner, J., Schmickl, T., and Crailsheim, K. (2010b). A hormone-based controller for evolutionary multi-modular robotics: From single modules to gait learning. In *Proceedings of the IEEE Congress on Evolutionary Computation (CEC'10)*. in press.

Holmes, S. (1903). Phototaxis in *volvox*. *Biological Bulletin*, 4(6):319–326.

Khan, S., Spudich, J. L., McCray, J. A., and Trentham, D. R. (1995). Chemotactic signal integration in bacteria. *Proceedings of the National Academy of Sciences*, 92:9757–9761.

Mondada, F., Bonani, M., Raemy, X., Pugh, J., Cianci, C., Klaptocz, A., Magnenat, S., Zufferey, J.-C., Floreano, D., and Martinoli, A. (2009). The e-puck, a robot designed for education in engineering. In *Proceedings of the 9th Conference on Autonomous Robot Systems and Competitions*, volume 1, pages 59–65.

Schmickl, T. and Crailsheim, K. (2009). Modelling a hormone-based robot controller. In *MATHMOD 2009 - 6th Vienna International Conference on Mathematical Modelling*.

Stradner, J., Hamann, H., Schmickl, T., and Crailsheim, K. (2009). Analysis and implementation of an artificial homeostatic hormone system: A first case study in robotic hardware. In *The 2009 IEEE/RSJ International Conference on Intelligent Robots and Systems (IROS'09)*, pages 595–600. IEEE Press.

Yi, T.-M., Huang, Y., Simon, M. I., and Doyle, J. (2000). Robust perfect adaptation in bacterial chemotaxis through integral feedback control. *Proceedings of the National Academy of Sciences*, 97(9):4649–4653.